Model Based Predictive Current Control for a Three-Phase Cascade H-Bridge Multilevel STATCOM Operating at Fixed Switching Frequency

L. Comparatore, R. Gregor, J. Rodas, J. Pacher and A. Renault
Laboratory of Power and Control Systems
Universidad Nacional de Asunción
Luque, Paraguay

M. Rivera
Department of Electrical Engineering
Universidad de Talca
Curicó, Chile

***Abstract*—The absence of modulator in model based predictive control technique for different converter topologies generates a variable switching frequency that produces high frequency harmonics and higher stress on the power semiconductor devices. In this paper, a novel model based predictive control strategy with a fixed switching frequency applied to a three-phase cascade H-bridge multilevel STATCOM is introduced with the aim to increase the performance of classical model predictive control. Simulation results show increased performance of the proposed control method in terms of current waveform total harmonic distortion.**

***Index Terms*—Cascade H-bridge converter, fixed switching frequency, model based predictive control.**

NOMENCLATURE

CHB	Cascade H-bridge.
MBPC	Model based predictive control.
MSE	Mean squared error.
PCC	Point of common coupling.
STATCOM	Static synchronous compensator.
THD	Total harmonic distortion.

I. INTRODUCTION

The major reasons for the growing interest in the use of MBPC technique are the evolution of data processing capabilities of the digital signal processors, its nonlinear operation, fast dynamic response and simplicity to represent different control objectives by a cost function. Classical MBPC method consists in use a precise mathematical model of the system to have an accurate prediction of the behavior of the controlled variables, where the prediction is carried out for each possible switching state, that in power converters, there are always a limited number of valid switching states. Next, an optimization process uses this information to evaluate a defined cost function for each prediction to provide the control action that minimizes such cost function. Then, the control action selected is applied in the next sampling time [1]. The classic MBPC has the particularity to provide a variable switching frequency, due to the absence of modulator. In terms of power quality, not only the spread spectrum and the high frequency harmonics are shown in the output waveforms but also the high stress on the power semiconductor devices. In order to solve these issues, a novel approach for different topologies and its applications has been presented: three-phase active rectifier [2], two-level voltage source inverters [3]-[5], direct matrix converters [6], [7], active power compensators [8], neutral pointed clamping converters [9] and 7-level CHB back-to-back converter [10]. Of all of the different topologies and their applications, the CHB multilevel converters-based is one of the most commonly used and an attractive topology due to their modularization, extensibility, control simplicity and high-quality output [11], [12].

The purpose of this paper is to use a MBPC strategy with fixed switching frequency, in order to control a three-phase CHB 7-level STATCOM. Noteworthy that the proposal is not innovative, however, still now is not recorded in the literature neither simulations results nor experimental results of this control technique applied to three-phase CHB 7-level converter for STATCOM applications. The proposed control approach consists in to include a modulation stage in the optimization algorithm of the classical MBPC, to generate the duty cycles for two active switching states and one null switching state which are applied to the CHB 7-level STATCOM using a switching pattern procedure. An optimization process considering a defined cost function allows calculating the duty cycles of each switching state.

II. CHB CONVERTER-BASED STATCOM MODEL

Fig. 1 shows the three-phase 7-level CHB converter-based STATCOM coupled to the power grid and the load through a shunt power filter (L_f-R_f), connected in the PCC. The STATCOM is composed by three cells H-bridge per phase with an independent DC-link for each cell. All DC-link buses have the same voltage v_{dc} and the same capacitance C_{dc} values. Each cell contains four switching devices which are activated with digital signals $s\phi_{ij}$, being ϕ the corresponding phase (a, b or c), i the cell number (1, 2 or 3) and j the switching device (1, 2, 3 or 4). With the purpose of avoiding a short-circuit in the DC-link, the signals $s\phi_{i1}$ and $s\phi_{i3}$ are complementary to $s\phi_{i2}$ and $s\phi_{i4}$ respectively. Then, to adjust

978-1-5090-5339-1/17/$31.00 © 2017 IEEE

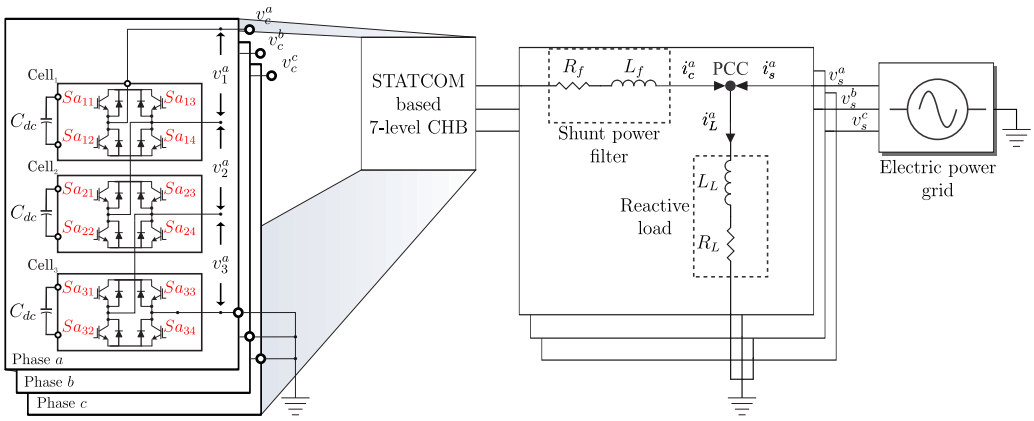

Fig. 1. Three-phase 7-level CHB converter-based STATCOM system connection.

the output voltage v_c^ϕ, only $2n_c = 6$ signals are needed. Each phase have $n_c = 3$ number of cells and $\varepsilon = 2^{2n_c} = 64$ possible switching states. Furthermore, each switching state corresponds to a switching function $F_s^\phi = \sum_{i=1}^{n_c} F_i^\phi$, where F_i^ϕ is the switching function for the cell i, whose possible values are shown in Table I.

TABLE I
SWITCHING FUNCTIONS FOR THE CELL "i"

$s\phi_{i1}$	$s\phi_{i3}$	$s\phi_{i2}$	$s\phi_{i4}$	F_i^ϕ
1	0	0	1	+1
1	1	0	0	0
0	0	1	1	0
0	1	1	0	−1

The output voltage can be synthesized as a function of the DC-link voltage v_{dc} and the switching function F_s^ϕ as:

$$v_c^\phi = F_s^\phi v_{dc} \tag{1}$$

Using Kirchhoff's circuit laws, the continuous time-domain model of the CHB converter-based STATCOM is:

$$\frac{\mathrm{d}i_c^\phi}{\mathrm{d}t} = \frac{v_s^\phi}{L_f} - \frac{R_f}{L_f} i_c^\phi - \frac{v_c^\phi}{L_f} \tag{2}$$

where i_c^ϕ is the current injected by the CHB converter-based STATCOM and v_s^ϕ the grid voltage.

The discrete time-domain model is obtained by using the forward-Euler discretization method:

$$i_c^\phi(k+1) = \left(1 - \frac{R_f T_s}{L_f}\right) i_c^\phi(k) + \frac{T_s}{L_f}\left\{v_s^\phi(k) - v_c^\phi(k)\right\} \tag{3}$$

being T_s the sampling time, k identifies the actual discrete-time sample and $i_c^\phi(k+1)$ are the predictions of the STATCOM phase currents made at sample k.

III. Proposed Predictive Control with Fixed Switching Frequency

The classical MBPC technique uses the predictive model represented by (3) to predict the behavior of the future states of all possible switching states. Then, the predicted errors for current tracking are calculated as follows:

$$ei_c^\phi(k+1) = i_c^{\phi^*}(k+1) - i_c^\phi(k+1) \tag{4}$$

where the superscript (*) indicates a reference variable.

The cost function (for each phase ϕ) is defined as a quadratic measure of the predicted error, as follows:

$$g^\phi = \| \, ei_c^\phi(k+1) \, \|^2 \tag{5}$$

where $\| \, . \, \|$ denotes the magnitude of the variable.

Finally, the switching state that generates the minimum value of the defined cost function is selected by an optimization process clearly described in the Algorithm 1. This optimum switching state is applied in the next sampling time during the whole switching period.

Algorithm 1 Optimization algorithm of the classic MBPC

1. Initialize $g_{opt}^a := \infty, g_{opt}^b := \infty, g_{opt}^c := \infty, \eta := 0$
2. Compute $i_c^{a^*}(k+1)$, $i_c^{b^*}(k+1)$ and $i_c^{c^*}(k+1)$
3. **while** $\eta \leq \varepsilon$ **do**
4. Compute $i_c^a(k+1)$, $i_c^b(k+1)$ and $i_c^c(k+1)$
5. Compute $ei_c^a(k+1)$, $ei_c^b(k+1)$ and $ei_c^c(k+1)$
6. Compute g^a, g^b and g^c
7. **if** $g^a < g_{opt}^a$ **then**
8. $g_{opt}^a \leftarrow g^a, \quad F_{s,opt}^a \leftarrow F_{s,\eta}^a$
9. **end if**
10. **if** $g^b < g_{opt}^b$ **then**
11. $g_{opt}^b \leftarrow g^b, \quad F_{s,opt}^b \leftarrow F_{s,\eta}^b$
12. **end if**
13. **if** $g^c < g_{opt}^c$ **then**
14. $g_{opt}^c \leftarrow g^c, \quad F_{s,opt}^c \leftarrow F_{s,\eta}^c$
15. **end if**
16. $\eta := \eta + 1$
17. **end while**

A. Classical vs. proposed MBPC

The main difference between the proposed method and the classical MBPC, is that the proposed method proceeds as

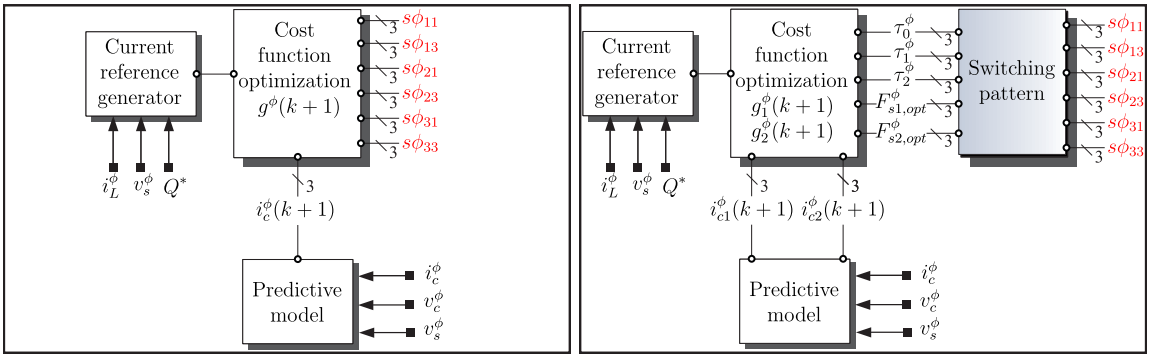

Fig. 2. Block diagram for: (a) the classic MBPC, (b) the proposed MBPC at fixed switching frequency.

space vector modulation. In space vector modulation, each sector is defined by two adjacent vectors (and one null vector), nonetheless, in this work, the "sectors" are defined by two consecutive active (or no-null) states and one null state (please refer to Appendix). For simplicity, always $\eta = 1$ is used as null state (where η is the state number, defined in the Appendix). Then, the first sector is the one between switching state number $\eta = 2$ and switching state number $\eta = 3$, the second sector, the one between switching state number $\eta = 3$ and switching state number $\eta = 5$, and so on. The two optimum states are chosen by an optimization process that evaluates the predicted errors separately for each prediction and are applied during specified times, being their duty cycles inversely proportional to the respective cost functions.

The block diagram of the classic MBPC method and the proposed method are shown in Fig. 2, where the switching pattern block is highlight.

B. Cost function optimization

The new cost function (for each phase ϕ) for the proposed method is defined as the sum of the cost functions $g_{1,2}^\phi$ defined by (5) whose respective weighting factors are the duty cycles $\tau_{1,2}^\phi$ for the two active states, leaving the equation as:

$$g^\phi = \tau_1^\phi g_1^\phi + \tau_2^\phi g_2^\phi \tag{6}$$

The switching state that generates the lowest value of the cost function must be applied higher time, i.e., the duty cycle must be inversely proportional to the cost function. The duty cycles for the two active switching states and one null switching state are calculated by solving:

$$\begin{aligned} \tau_0^\phi &= K^\phi / g_0^\phi \\ \tau_1^\phi &= K^\phi / g_1^\phi \\ \tau_2^\phi &= K^\phi / g_2^\phi \\ \tau_0^\phi + \tau_1^\phi + \tau_2^\phi &= 1 \end{aligned} \tag{7}$$

where τ_0^ϕ correspond to the duty cycle of a null state which is evaluated only one time and K^ϕ is the constant of proportionality.

The expressions of the duty cycles for each switching state are given solving (7) for K^ϕ as:

$$\begin{aligned} \tau_0^\phi &= g_1^\phi g_2^\phi / \left(g_0^\phi g_1^\phi + g_1^\phi g_2^\phi + g_0^\phi g_2^\phi \right) \\ \tau_1^\phi &= g_0^\phi g_2^\phi / \left(g_0^\phi g_1^\phi + g_1^\phi g_2^\phi + g_0^\phi g_2^\phi \right) \\ \tau_2^\phi &= g_0^\phi g_1^\phi / \left(g_0^\phi g_1^\phi + g_1^\phi g_2^\phi + g_0^\phi g_2^\phi \right) \end{aligned} \tag{8}$$

Being the turn-on times (T_0^ϕ, T_1^ϕ and T_2^ϕ) the products of multiplying the duty cycles (τ_0^ϕ, τ_1^ϕ and τ_2^ϕ) by the sampling time, respectively.

Finally, the optimization process (for each phase ϕ) is illustrated in Algorithm 2.

Algorithm 2 Optimization algorithm of the proposed method

1. Initialize $g_{opt}^\phi := \infty, \eta := 0$
2. Compute $i_c^*(k+1)$
3. Compute $i_{c\,0}^\phi(k+1)$
4. Compute $ei_{c\,0}^\phi(k+1)$
5. Compute $g_0^\phi = g_0^\phi(k+1)$
6. **while** $\eta \leq \varrho$ **do**
7. Compute $i_{c\,1}^\phi(k+1)$ and $i_{c\,2}^\phi(k+1)$
8. Compute $ei_{c\,1}^\phi(k+1)$ and $ei_{c\,2}^\phi(k+1)$
9. Compute $g_1^\phi = g_1^\phi(k+1)$ and $g_2^\phi = g_2^\phi(k+1)$
10. Compute τ_0^ϕ, τ_1^ϕ and τ_2^ϕ
11. Compute $g^\phi = \tau_1^\phi g_1^\phi + \tau_2^\phi g_2^\phi$
12. **if** $g^\phi < g_{opt}^\phi$ **then**
13. $g_{opt}^\phi \leftarrow g^\phi$
14. Compute T_0^ϕ, T_1^ϕ and T_2^ϕ
15. $F_{s1,opt}^\phi \leftarrow F_{s1,\eta}^\phi, F_{s2,opt}^\phi \leftarrow F_{s2,\eta}^\phi$
9. **end if**
10. $\eta := \eta + 1$
11. **end while**

C. Switching pattern

At the end of the optimization process, the two optimum active switching states ($F_{s1,opt}^\phi$ and $F_{s2,opt}^\phi$) and the one null switching state are applied during their respective turn-on

times using the switching pattern procedure that is shown in Fig. 4, similar to [3], [4].

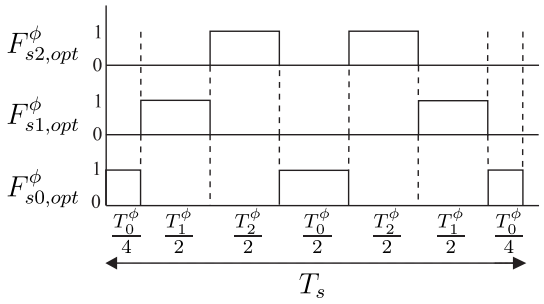

Fig. 3. Switching pattern for the optimal switching states.

D. Current reference generator

Using the following Clarke's transformation matrix:

$$\mathbf{T} = \sqrt{\frac{2}{3}} \begin{bmatrix} 1 & -\frac{1}{2} & -\frac{1}{2} \\ 0 & \frac{\sqrt{3}}{2} & -\frac{\sqrt{3}}{2} \\ \frac{1}{\sqrt{2}} & \frac{1}{\sqrt{2}} & \frac{1}{\sqrt{2}} \end{bmatrix} \tag{9}$$

the instantaneous $\alpha - \beta$ current references are:

$$\begin{bmatrix} i_c^{\alpha^*} \\ i_c^{\beta^*} \end{bmatrix} = \frac{1}{(v_s^{\alpha})^2 + (v_s^{\beta})^2} \begin{bmatrix} v_s^{\alpha} & v_s^{\beta} \\ v_s^{\beta} & -v_s^{\alpha} \end{bmatrix} \begin{bmatrix} P_c^* \\ Q_c^* \end{bmatrix} \tag{10}$$

where the instantaneous active and reactive power references ideally are:

$$\begin{aligned} P_c^* &= 0 \\ Q_c^* &= -Q_L \end{aligned} \tag{11}$$

being $Q_L = v_{s\alpha} i_{L\beta} - v_{s\beta} i_{L\alpha}$ the instantaneous reactive load power to be compensate.

Finally, the STATCOM phase currents references used in the optimization process are:

$$[i_c^{a^*} \quad i_c^{b^*} \quad i_c^{c^*}]' = \mathbf{T}^{-1} [i_c^{\alpha^*} \quad i_c^{\beta^*} \quad 0]' \tag{12}$$

where the superscript $(')$ indicates the transposed matrix.

IV. Simulation Results

In order to validate the effectiveness of the proposed method, simulation results in Matlab/Simulink environment were carried out, considering the electrical parameters shown in Table II. The performance of the proposed method are compared with the results obtained with the classical MBPC implementation, in both cases considering a 25 kHz of sampling frequency.

A good current tracking is presented in Fig. 4 (upper), having a reduction in the MSE from 0.4206 A to 0.3207 A. Moreover, in Fig. 4 (bottom) it is possible to notice how the instantaneous reactive power is compensated ($Q_c = -Q_L$). The big spikes are consequence of the application of the null vector in the switching pattern.

TABLE II
Parameters Description

PARAMETER	SYMBOL	VALUE	UNIT
	Electric power grid		
Grid frequency	f_e	50	Hz
Grid voltage	v_s	310.2	V
	7-Level CHB STATCOM		
Filter resistance	R_f	0.09	Ω
Filter inductance	L_f	3	mH
DC-link voltage	v_{dc}	154	V
	Load parameters		
Load resistance	R_L	23.2	Ω
Load inductance	L_L	55	mH
	Predictive control parameters		
Sampling time	T_s	40	μs
Simulation step	–	1	μs

A comparison analysis between the proposed method and the classical MBPC is shown in Fig. 5 considering; (upper) the switching pattern, (middle) the output voltages of the STATCOM and (bottom) the THD of the analyzed output voltage. As shown in Fig. 5 (b) a more sinusoidal output voltage v_c^a is obtained with respect to the output voltage than in Fig. 5 (a) due to the switching pattern procedure. Furthermore, the operation at fixed switching frequency produces a more concentrated spectrum in exchange of a higher THD parameter of the output voltage (due to the way in which the sectors were defined).

Additionally, considering the interval 0.05 to 0.09 s, Fig. 6 shows the improvement obtained in the THD performance parameter of the grid current, that is about 65% (a drop from 6.61% to 2.32%) using the proposed method.

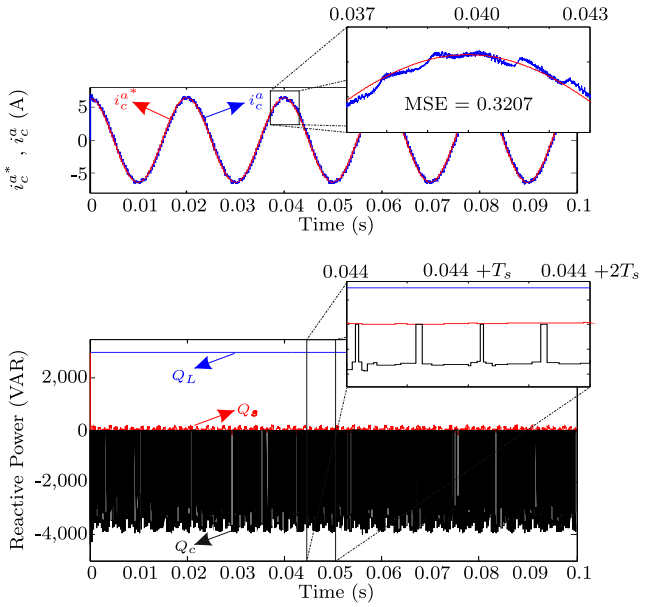

Fig. 4. CHB STATCOM response: (upper) current tracking, (bottom) reactive power compensation.

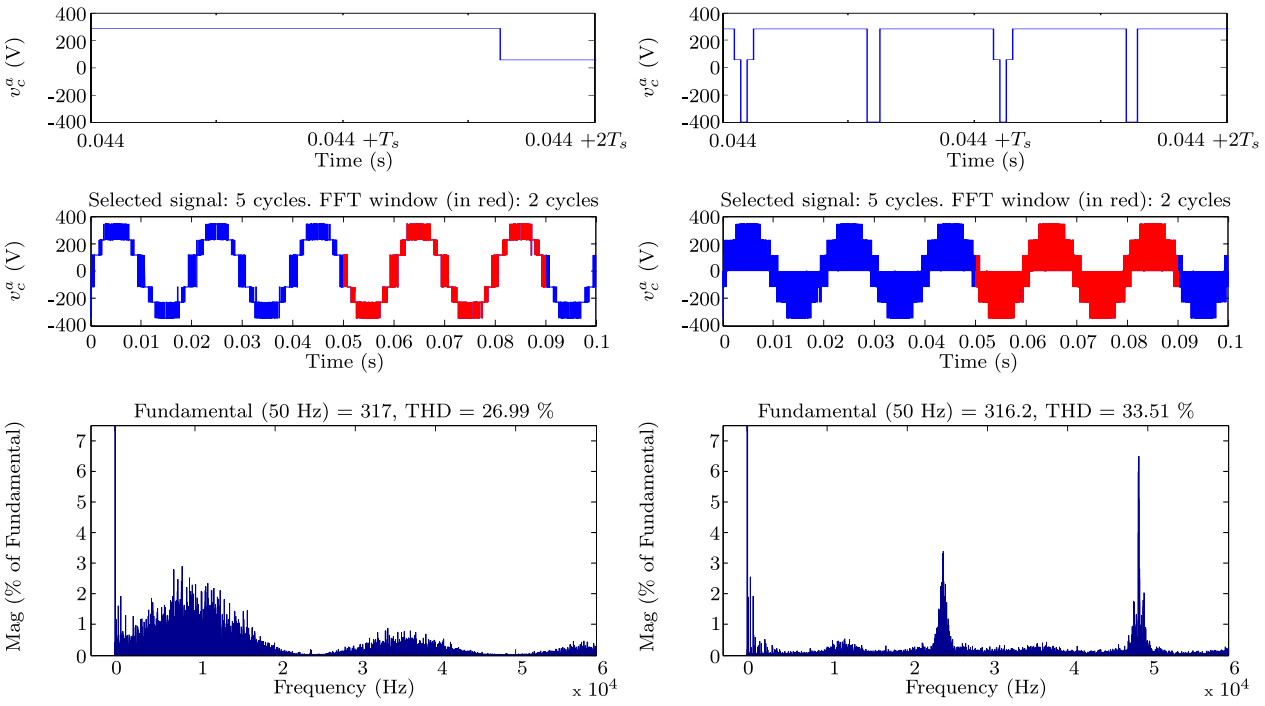

(a) Classical MBPC response

(b) Proposed MBPC at fixed switching frequency response

Fig. 5. Comparison performance considering: (upper) the switching pattern of the output voltage of the STATCOM obtained (middle) the output voltage of the STATCOM and (bottom) the THD of the output voltage.

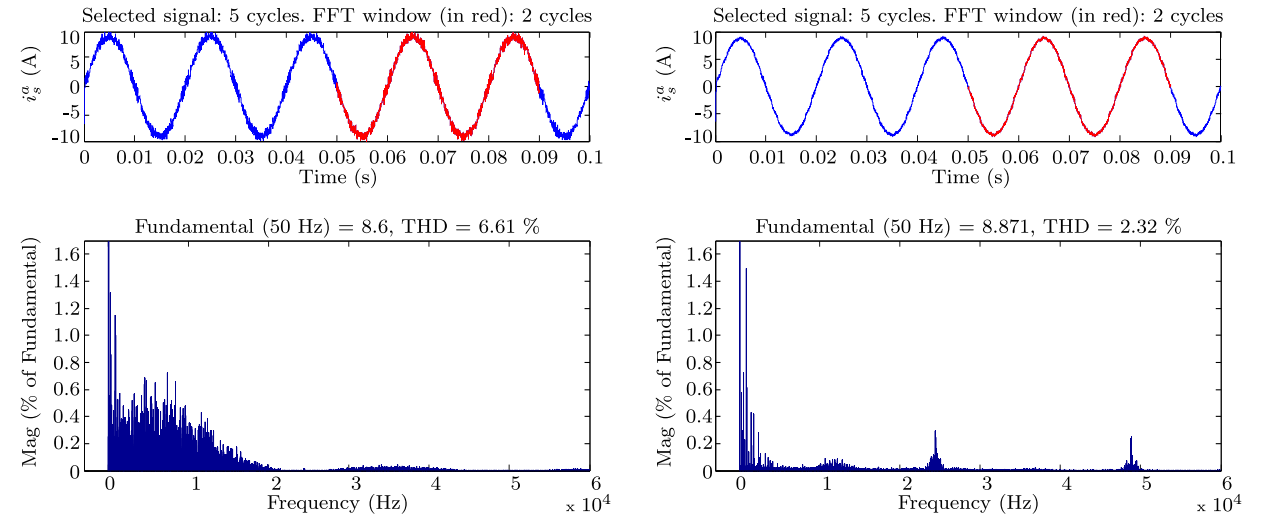

(a) Classical MBPC response

(b) Proposed MBPC at fixed switching frequency response

Fig. 6. Comparison performance considering: (upper) the grid current and (bottom) the THD of the grid current.

V. Conclusion

In this paper, a MBPC operating at fixed switching frequency applied to the three-phase CHB 7-level STATCOM has been proposed. From the simulation results it is possible to confirm a good capability of the proposed control technique to compensate the reactive power and better performance in terms of THD and MSE, compared with the results obtained by the classical MBPC. A comparative simulation results performed with reference to the classical predictive control also show improvements relative to the output voltage waveform.

Acknowledgment

The authors would like to thank to the Paraguayan Government for the economical support they provided through the CONACYT Grant 14-INV-096. This work was also made possible by the FONDECYT Regular Project N° 1160690.

References

[1] S. Kouro, M. A. Perez, J. Rodriguez, A. M. Llor, and H. A. Young, "Model predictive control: MPC's role in the evolution of power electronics," *IEEE Ind. Electron. Mag.*, vol. 9, no. 4, pp. 8–21, 2015.

[2] L. Tarisciotti, P. Zanchetta, A. Watson, J. C. Clare, M. Degano, and S. Bifaretti, "Modulated model predictive control for a three-phase active rectifier," *IEEE Trans. Ind. Electron.*, vol. 51, no. 2, pp. 1610–1620, 2015.

[3] M. Rivera, F. Morales, C. Baier, J. Muoz, L. Tarisciotti, P. Zanchetta, and P. Wheeler, "A modulated model predictive control scheme for a two-level voltage source inverter," in *Proc. ICIT*, Seville, 2015, pp. 2224–2229.

[4] M. Rivera, "A new predictive control scheme for a VSI with reduced common mode voltage operating at fixed switching frequency," in *POWERENG*, Riga, 2015, pp. 617–622.

[5] M. Tomlinson, T. Mouton, and R. Kennel, "Finite-control-set model predictive control with a fixed switching frequency vs. linear control for current control of a single-leg inverter," in *Proc. PRECEDE*, Valparaiso, 2015, pp. 109–114.

[6] M. Vijayagopal, P. Zanchetta, L. Empringham, L. D. Lillo, L. Tarisciotti, and P. Wheeler, "Modulated model predictive current control for direct matrix converter with fixed switching frequency," in *Proc. EPE ECCE-Europe*, Geneva, 2015, pp. 1–10.

[7] M. Vijayagopal, L. Empringham, L. de Lillo, L. Tarisciotti, P. Zanchetta, and P. Wheeler, "Current control and reactive power minimization of a direct matrix converter induction motor drive with modulated model predictive control," in *Proc. PRECEDE*, Valparaiso, 2015, pp. 103–108.

[8] R. Rabbeni, L. Tarisciotti, A. Gaeta, A. Formentini, P. Zanchetta, M. Pucci, M. Degano, and M. Rivera, "Finite states modulated model predictive control for active power filtering systems," in *Proc. IEEE ECCE*, Montreal, 2015, pp. 1556–1562.

[9] M. Norambuena, H. Yin, S. Dieckerhoff, and J. Rodriguez, "Improved finite control set model predictive control with fixed switching frequency for three phase NPC converter," in *Proc. PCIM Europe*, Nuremberg, Germany, 2016, pp. 1–8.

[10] L. Tarisciotti, P. Zanchetta, A. Watson, S. Bifaretti, and J. C. Clare, "Modulated model predictive control for a seven-level cascaded H-bridge back-to-back converter," *IEEE Trans. Ind. Electron.*, vol. 61, no. 10, pp. 5375–5383, 2014.

[11] R. Gregor, A. Renault, L. Comparatore, J. Pacher, J. Rodas, D. Gregor, J. Muñoz, and M. Rivera, "Finite-states model predictive control with increased prediction horizon for a 7-level cascade H-bridge multilevel STATCOM," in *Proc. WMSCI*, Miami, 2016, pp. 1–6, CD–ROM.

[12] R. Gregor, L. Comparatore, A. Renault, J. Rodas, J. Pacher, S. Toledo, and M. Rivera, "A novel predictive-fixed switching frequency technique for a cascade H-Bridge multilevel STATCOM," in *Proc. IECON*, Florence, 2016, pp. 3672–3677.

Appendix

TABLE III
Switching functions for a three-phase 7-level CHB converter-based STATCOM system

$S\phi_\eta$						η	$F^{\phi}_{s,\eta}$
$s\phi_{11}$	$s\phi_{13}$	$s\phi_{21}$	$s\phi_{23}$	$s\phi_{31}$	$s\phi_{33}$		
0	0	0	0	0	0	1	0
0	0	0	0	0	1	2	-1
0	0	0	0	1	0	3	1
0	0	0	0	1	1	4	0
0	0	0	1	0	0	5	-1
0	0	0	1	0	1	6	-2
0	0	0	1	1	0	7	0
0	0	0	1	1	1	8	-1
0	0	1	0	0	0	9	1
0	0	1	0	0	1	10	0
0	0	1	0	1	0	11	2
0	0	1	0	1	1	12	1
0	0	1	1	0	0	13	0
0	0	1	1	0	1	14	-1
0	0	1	1	1	0	15	1
0	0	1	1	1	1	16	0
0	1	0	0	0	0	17	-1
0	1	0	0	0	1	18	-2
0	1	0	0	1	0	19	0
0	1	0	0	1	1	20	-1
0	1	0	1	0	0	21	-2
0	1	0	1	0	1	22	-3
0	1	0	1	1	0	23	-1
0	1	0	1	1	1	24	-2
0	1	1	0	0	0	25	0
0	1	1	0	0	1	26	-1
0	1	1	0	1	0	27	1
0	1	1	0	1	1	28	0
0	1	1	1	0	0	29	-1
0	1	1	1	0	1	30	-2
0	1	1	1	1	0	31	0
0	1	1	1	1	1	32	-1
1	0	0	0	0	0	33	1
1	0	0	0	0	1	34	0
1	0	0	0	1	0	35	2
1	0	0	0	1	1	36	1
1	0	0	1	0	0	37	0
1	0	0	1	0	1	38	-1
1	0	0	1	1	0	39	1
1	0	0	1	1	1	40	0
1	0	1	0	0	0	41	2
1	0	1	0	0	1	42	1
1	0	1	0	1	0	43	3
1	0	1	0	1	1	44	2
1	0	1	1	0	0	45	1
1	0	1	1	0	1	46	0
1	0	1	1	1	0	47	2
1	0	1	1	1	1	48	1
1	1	0	0	0	0	49	0
1	1	0	0	0	1	50	-1
1	1	0	0	1	0	51	1
1	1	0	0	1	1	52	0
1	1	0	1	0	0	53	-1
1	1	0	1	0	1	54	-2
1	1	0	1	1	0	55	0
1	1	0	1	1	1	56	-1
1	1	1	0	0	0	57	1
1	1	1	0	0	1	58	0
1	1	1	0	1	0	59	2
1	1	1	0	1	1	60	1
1	1	1	1	0	0	61	0
1	1	1	1	0	1	62	-1
1	1	1	1	1	0	63	1
1	1	1	1	1	1	64	0